Potassium Capture by Kaolin, Part 2: K_2CO_3, KCl, and K_2SO_4

Wang, Guoliang; Jensen, Peter Arendt; Wu, Hao; Jappe Frandsen, Flemming; Sander, Bo; Glarborg, Peter

Published in:
Energy and Fuels

Link to article, DOI:
10.1021/acs.energyfuels.7b04055

Publication date:
2018

Document Version
Peer reviewed version

Potassium Capture by Kaolin, Part 2: K_2CO_3, KCl and K_2SO_4

Guoliang Wang,[*†] Peter Arendt Jensen,[†] Hao Wu,[†] Flemming Jappe Frandsen,[†] Bo Sander,[‡] Peter Glarborg[†]

[†]Department of Chemical and Biochemical Engineering, Technical University of Denmark, Søltofts Plads, Building 229, DK-2800 Lyngby, Denmark

[‡]Ørsted Bioenergy & Thermal Power A/S, Kraftværksvej 53, 7000 Fredericia, Denmark

Keywords: Kaolin, potassium-capture, biomass combustion, additive, KCl, K_2SO_4

***Corresponding author email-id:** guow@kt.dtu.dk

Abstract: The reaction of kaolin powder with K_2CO_3, KCl and K_2SO_4 at suspension-fired conditions was studied by entrained flow reactor experiments and equilibrium calculations. The influence of reaction temperature, K-concentration in the flue gas, molar ratio of K/(Al+Si) in the reactants, and gas residence time on the reaction was investigated. The results showed that the K-capture level (C_K) (g potassium reacted by per g kaolin available) of K_2CO_3 and KCl by kaolin generally followed the equilibrium predictions at temperatures above 1100 °C, when using a kaolin particle size of D_{50} = 5.47 μm and a residence time of 1.2 s. This revealed that a nearly full conversion was obtained without kinetic or transport limitations at the conditions applied. At 800 and 900 °C, the

measured conversions were lower than the equilibrium predictions, indicating that the reactions were either kinetically or diffusion controlled. The measured C_K of K_2SO_4 by kaolin was much lower than the equilibrium predictions. Kaliophilite ($KAlSiO_4$) product was predicted by the equilibrium calculations of the K_2SO_4 capture reaction; however the XRD results revealed that leucite ($KAlSi_2O_6$) was formed. Compared with the C_K of KOH reacting with kaolin, the C_K of K_2CO_3 was similar, while the C_K value of KCl and K_2SO_4 were both lower.

1 Introduction

The Danish government plans to phase out coal from power plants by 2030, mainly through promoting wind energy and replacing coal with biomass in power plants.[1] Suspension-firing of biomass can provide CO_2-neutral electricity with higher efficiency compared to traditional grate-firing.[2] However, ash-related problems have sometimes hampered the utilization of biomass in suspension-fired power plants.

Potassium is present naturally in plant materials and it is the main cause for most ash-related problems,[3-6] including deposition,[7-10] corrosion[11, 12] and SCR catalyst deactivation in biomass-fired boilers.[13-15] During biomass combustion, potassium is released to gas phase in different forms depending on the ash chemistry of the fuels and combustion conditions. K-species including KOH, K_2CO_3, KCl and K_2SO_4 have been detected in the ash from biomass-fired boilers.[3, 16-22] In the combustion of woody biomass with a low fuel Cl and S content, potassium may appear as K_2CO_3 and KOH in the flue gas.[23] However, when Cl and S are available, like in the case of herbaceous biomass combustion, KCl and K_2SO_4 become the dominant K-containing compounds.[23, 24] KCl and K_2SO_4 have melting temperatures of around 770 °C and 850 °C, respectively. The binary system of KCl and K_2SO_4

may melt at as low as 690 °C forming sticky surface on heat transfer surfaces.[25] The melted K-salts can function as a glue and accelerate the formation of ash deposit. Additionally, the deposited KCl can cause severe corrosion.[26] When the flue gas is cooled down, the condensation of KCl and K_2SO_4 forms aerosols that can poison SCR de-NO_x catalysts and thereby impede the plant NO_x removal system.[13-15] The efficiency and availability of biomass-fired boilers can be decreased due to problems caused by the potassium-rich biomass ash.[27-29]

Injecting additives to capture and transfer the volatile potassium species into less corrosive compounds with a higher melting point is an option to reduce biomass ash related challenges.[17, 30-32] Kaolin and coal fly ash have been identified as effective potassium-capture additives for biomass combustion.[33, 34] Kaolin is a kind of clay that is rich in a layered aluminosilicate mineral – kaolinite ($Al_2Si_2O_5(OH)_4$). Coal fly ash often contains mullite ($3Al_2O_3{\cdot}2SiO_2$) as the main mineral phase.[35] Kaolinite and mullite can react with volatile alkali species and bind alkali in alkali-aluminosilicate species.[17, 36]

When kaolin is heated, it decomposes and transfers into metakaolin above 450 °C.[37, 38] Metakaolin can capture gaseous potassium species such as KOH, KCl and K_2SO_4. Using KCl as an example, metakaolin react with KCl forming K-aluminosilicate, releasing HCl into the gas phase, see reaction R1 and R2.[39-41] K-aluminosilicate has a higher melting point compared to KOH, KCl and K_2SO_4 and thereby the potassium becomes less problematic for the boiler operation. Coal fly ash with mullite as the main mineral phase, can react with volatile K-species in a similar way as kaolin.[17, 42-46]

$$Al_2O_3 \cdot 2SiO_2(metakaolin) + 2KCl + H_2O \rightarrow 2KAlSiO_4(kalsilite/kaliophilite) + 2HCl\ (g) \quad \text{(R 1)}$$

$$Al_2O_3 \cdot 2SiO_2(metakaolin) + 2SiO_2 + 2KCl + H_2O \rightarrow 2KAlSi_2O_6\ (leucite) + 2HCl(g) \quad \text{(R 2)}$$

Kaolin has been tested in a large-scale CFB boilers as an additive to prevent alkali-related problems.[47] With the addition of kaolin, the amount of water soluble K and Cl in the fly ash was significantly decreased, and the bed agglomeration temperature was increased.[47] Coal fly ash has been commercially utilized in full-scale biomass suspension-fired boilers in Denmark.[17, 30, 48] In order to optimize the use of these additives in biomass suspension-fired boilers, a thorough understanding of the reaction of these additives with different volatile potassium species is wanted.

Alkali capture by kaolin has been studied previously.[36, 39, 40, 49-51] Shadman and co-workers studied the reaction of gaseous NaCl and KCl with kaolin flakes in a fixed bed reactor. [32, 36, 49, 52, 53] The results showed that kaolin captured NaCl and KCl irreversibly through chemical reaction. The reaction was diffusion-influenced under the studied conditions (800 °C, kaolin flakes with a thickness of 0.5 mm, and a residence time of 40 hours). A weight increase of 26.6 % of saturated kaolin flakes was observed by the NaCl-kaolin reaction.[32]

In the study by Zheng et al.,[50] the kinetics of gaseous KCl capture by kaolin pellets with a diameter of 1.5 mm was investigated in a fixed bed reactor. The influence of oxygen content (0 - 20 %), water content (0 - 3 vol. %), KCl concentration (0 - 1600 ppmv), as well as the reaction temperature (900 - 1500 °C) on the reaction was studied. It was shown that the diffusion of KCl inside the kaolin pellets was the rate-controlling step of the reaction at the studied conditions. The reaction temperature posed a significant impact on the KCl-capture reaction under the studied conditions. The K-capture level of kaolin decreased with exposure temperature up to 1300 °C and then increased with further increasing the exposure temperature to 1500 °C. This is because at 900-1300 °C, sintering of kaolin pellets took place, resulting in a gradual replacement of fast gas diffusion by slow condensed-state diffusion. At

temperatures above 1300 °C, a partially molten phase was formed inside the pellets; as a result the liquid diffusion improved the transport of KCl.[50]

In a fixed bed study by Tran et al.,[39-41] the K-capture reaction by kaolin flakes with a diameter of 0.5-2 mm was studied in a fixed bed reactor equipped with an alkali detector. The reaction temperature was in the range of 750-950 °C. The results revealed that potassium is captured by kaolin not only via chemical adsorption, but also physical adsorption. The comparison of results using KOH, KCl and K_2SO_4 show that the total absorption rate of KCl by kaolin was slightly higher than that of KOH, while the absorption rate of K_2SO_4 was significantly lower than that of KOH and KCl at the studied conditions.

The studies mentioned above were all conducted in fixed bed reactors where kaolin was present in the form of pellets or flakes, and the reaction time was as long as hours. The reaction conditions differ significantly from those in suspension fired boilers, where kaolin particles are well dispersed and the reaction time is only a few seconds.[30, 54] Additionally, alkali species and kaolin may be exposed to flame temperature as high as 1700 °C.[27, 54] The reaction of K-species with kaolin at suspension-firing conditions takes place between condensed-phase kaolin particles (solid or melted) and the gaseous potassium species.[55, 56] The reaction may be influenced by external and internal diffusion, kinetic limitations and chemical equilibrium.[39, 50] To the authors' knowledge, quantitative study on K-capture by kaolin at suspension-fired conditions is not available, and no previous study is published where the influence of alkali species (KCl, KOH, K_2CO_3 and K_2SO_4) on the reaction with kaolin at suspension-fired conditions is investigated and compared.

Wendt and co-workers studied the gaseous sodium capture reaction by kaolin at suspension fired conditions using a 17-kW down flow combustor. The results showed that the capture rate of NaOH was obviously higher than that of NaCl. They proposed that NaOH was the only reacting species in both

cases.[51, 57] However, whether the kinetics of Na-species and K-species capture by kaolin are the same has not been established.

In paper 1 of this paper series,[58] we have investigated the reaction between KOH and kaolin at suspension-fired conditions in the temperature range of 800 - 1450 °C. It was shown that 1g kaolin reacting with gas phase KOH can capture up to 0.22 g K in the temperature range of 1100 - 1300 °C, with a kaolin particle size of D_{50} = 5.47 μm and a residence time of 1.2 s. At the applied conditions, the KOH conversion could be reasonably predicted by equilibrium calculations at temperatures above 1100 °C.[58]

This is paper 2 of this paper series, investigating the reaction of kaolin with different K-species. The aim of this work is to get a thorough understanding of the K-capture reaction by kaolin under suspension-firing conditions so as to minimize or avoid ash-related problems caused by K-species during combustion of K-rich biomass fuels. More specifically, the objective of this work is to understand the influences of the molar ratio of K/(Al+Si) in reactants, K-concentration, reaction temperature and K-species type on the K-capture reaction using kaolin at suspension-firing conditions.

2 Experimental section

2.1 Materials

Kaolin powder purchased from VWR Chemicals was utilized in this study. The characteristics of the kaolin powder including elemental composition, particle size and BET surface area are listed in Table 1. It is seen that the molar (Na + K)/(Si + Al) ratio of the kaolin is 0.02, indicating a large fraction of Al and Si is available for K-capture. Additionally, the kaolin sample was analyzed by XRD (X-ray

Diffraction), and the results showed that kaolinite ($Al_2Si_2O_5(OH)_4$) was the main mineral phase with also some quartz (SiO_2).

2.2 Setup

Experiments were carried out in the DTU Entrained Flow Reactor (EFR), which can simulate the conditions in suspension-fired boilers. A schematic figure of the EFR can be found in Paper 1 of the paper series.[58] The vertical reactor tube of the EFR is 2 m long, with an inner diameter of 79 mm. The reactor can be electrically heated up to 1450 °C by 7 heating elements. A 0.8 m long preheater is above the vertical reactor tube for preheating the secondary gas. The potassium species (including K_2CO_3, KCl, and K_2SO_4) and kaolin were mixed with deionized water, to make a homogeneous slurry. The slurry was pumped into the EFR and subsequently atomized by the preheated secondary gas. The potassium species vaporized and reacted with kaolin in the reactor tube, and the solid products were collected by a cyclone (cut-off diameter of 2.3 μm) and a metal filter (pore size of 0.8 μm). Detailed information about the reactor can be found in paper 1 of this paper series.[58]

2.3 Experimental matrix

Two series of experiments were conducted in the EFR: K-salt vaporization experiments and K-salt capture experiments using kaolin. The experimental conditions are summarized in Table 2. In the K-salt vaporization experiments (series A in Table 2), solutions of K_2CO_3, KCl and K_2SO_4 respectively were fed into the EFR without kaolin, to study the vaporization and transformation of K_2CO_3, KCl and K_2SO_4 at high temperatures. The concentration of KCl was kept at 500 ppmv, while K_2CO_3 and K_2SO_4 were kept at 250 ppmv to maintain the same K-concentration in the flue gas. The solid samples in the cyclone and filter were carefully collected, weighted and stored for further analysis.

In the K-capture experiments (series B-H in Table 2), KCl, K_2CO_3 and K_2SO_4 were fed into the EFR together with kaolin, respectively. The impact of K-concentration, molar ratio of K/(Al+Si) in reactants, reaction temperature, and gas residence time on the K-capture reaction was investigated. In the K-capture experiments, the concentration of kaolin in the flue gas inside the EFR was kept constant. While the concentration of K-salts in the flue gas was varied, and the molar K/(Al+Si) ratio in the reactants changed consequently. The K-concentration in the flue gas was varied from 50 ppmv to 1000 ppmv, and the molar K/(Al+Si) ratio in the reactants changed from 0.048 to 0.961 correspondingly. For each experiment, solid products were carefully collected from the cyclone and filter. The representativeness of the collected solid samples was examined by comparing the molar ratios of K/(Al+Si) in collected solid samples with that of the fed reactants.

2.4 Analytical methods

The reacted solid samples from the K-capture experiments were analyzed with ICP-OES (Inductively Coupled Plasma Atomic Emission Spectroscopy) to determine the amount of potassium captured by kaolin. Two parameters were defined for the quantification: X_K (K-conversion), and C_K (K-capture level). X_K is defined as the percentage (%) of potassium in the input potassium species chemically captured by kaolin forming water-insoluble K-aluminosilicate. C_K is the mass of potassium captured by 1 g additive (kaolin) (g K/g additive). The details about the calculation methods can be found in paper 1 of this series of study.[58]

To characterize the mineralogical composition of the reacted solid products, water-washed solid products were subjected to X-ray diffractometry (XRD) analysis. The XRD patterns were determined with a Huber diffractometer with characteristic Cu Kα radiation and operation conditions of 40 kV and

40 mA. The identification of main crystalline phases was performed with the JADE 6.0 software package (MDI Livermore, CA) and diffraction database of PDF2-2004.

2.5 Equilibrium Calculation

To better understand the K-capture reaction by kaolin, equilibrium calculations were carried out using Factsage 7.0. The databases of FactPS, FToxid FTsalt and FTpulp were employed for the calculations. Information about the different data bases can be found in literature,[59, 60] and a detailed description of the equilibrium calculation is available in Appendix II of the supporting information.

3 Results and discussion

3.1 Vaporization and transformation of K-salts

The vaporization and transformation of K_2CO_3, KCl, and K_2SO_4 at high temperatures may affect the K-capture reaction, and it was studied at the conditions shown in series (A) of Table 2. K-species (K_2CO_3, KCl and K_2SO_4) entered into the EFR in a form of slurry droplets. When water in these droplets evaporated, condensed phase K-salts were formed, which could be vaporized to gas phase or stay as condensed phase in the reactor. If all the K-salts are vaporized, aerosols will be formed and captured only by the filter. If the K-salts are not fully vaporized, the condensed K-salts can generate some larger particles being collected by the cyclone. The mass fraction of the solid samples collected in the cyclone and filter is shown in Figure 1 (A, B and C). Results of corresponding equilibrium calculations were shown in Figure 1 (D, E, and F).

For K_2CO_3, the experimental results reveal that, at temperatures ≥ 1100 °C, all solid samples were captured by the filter, implying a complete vaporization was obtained. At 800 °C and 900 °C, 1.6 % and 2.7 % of the product samples was captured by the cyclone, respectively. An increase of CO_2

concentration by 262 ppmv in flue gas was observed at 1100 °C and above, corresponding to a complete decomposition of K_2CO_3 forming KOH and CO_2. This also indicates that the formation of K_2CO_3 during the gas cooling process is negligible, probably due to the fast cooling rate and the short residence time. At 800 and 900 °C, the CO_2 concentration increased by 122 ppmv and 213 ppmv, showing a decomposition fraction of 48.8 % and 85.2 %, respectively. However, XRD analysis of the collected solid samples showed that $K_2CO_3 \cdot 1.5H_2O$ is the only solid product collected from the K_2CO_3 vaporization experiments. The results imply that, the KOH aerosols collected by the metal filter probably reacted with CO_2 and moisture during the process of collecting, storage or delivery for XRD analysis, forming $K_2CO_3 \cdot 1.5H_2O$.

The KCl vaporization experiments show that all samples were collected in the filter at temperatures above 1100 °C, implying a complete vaporization of KCl at 1100 °C. At 800 and 900 C, 4.6 % and 2.5 % of the product solid samples were collected in the cyclone. The equilibrium calculations on KCl showed that at temperatures above 740 °C, potassium appeared mainly as gaseous KCl. Above 800 °C, some KOH appeared but gaseous KCl remained the dominant K-species. Solid samples collected from KCl vaporization experiments were analyzed with XRD and showed that all collected products were KCl, with no potassium carbonate or potassium hydrate detected.

The equilibrium calculation results showed that the melting point of K_2SO_4 was 1070 °C, and KOH starts to form at 900 °C. At 900-1070 °C, solid, gaseous K_2SO_4 and gaseous KOH co-existed, while at 1070-1220 °C, liquid, gaseous K_2SO_4 and gaseous KOH co-existed, with gaseous K_2SO_4 being the dominant species. At temperatures 1200-1800 °C, gaseous KOH became the major K-species. The mass distribution of the solid samples collected from K_2SO_4 vaporization experiments is illustrated in Figure 1 (C). It shows that more than 99 % of the solid samples were collected from the filter above 1100 °C. However the filter fraction is obviously lower at 800 °C and 900 °C, as 91 % and 95 %

respectively, indicating a lower degree of K_2SO_4 vaporization. The XRD analysis of the solid product samples shows that only K_2SO_4 was present, although a decomposition of K_2SO_4 forming KOH and SO_3/SO_2 was predicted by the equilibrium calculations. This is probably because K_2SO_4 was reformed rapidly during the cooling down process. This can also explain the fact that no SO_2 was detected in the flue gas during the K_2SO_4 vaporization experiments.

3.2 K_2CO_3 capture by kaolin

Equilibrium calculation

The equilibrium calculation results of K_2CO_3 capture by kaolin at 50-1000 ppmv K (25-500 ppmv K_2CO_3) in flue gas showed that the K-capture behavior of K_2CO_3 was the same as that of KOH.[58] Detailed results can be found in Appendix II of the supporting information. This is because at high temperatures K_2CO_3 decomposed forming KOH and CO_2, and then the formed KOH reacted with kaolin.

Impact of potassium concentration

The experimental results of K_2CO_3 capture by kaolin at different K-concentrations at 1100 °C are compared with the equilibrium calculation results in Figure 2. The experimental C_K and X_K generally followed the equilibrium predictions. The C_K increased from 0.019 g K/(g additive) to 0.216 g K/(g additive) when the K_2CO_3 concentration increased from 25 ppmv to 250 ppmv (molar ratio of K/(Al+Si) in reactants changed from 0.048 to 0.481), with X_K staying almost constant, at around 82.0 %. When the concentration of K_2CO_3 increased further to 375 ppmv (K/(Al+Si) = 0.721) and 500 ppmv (K/(Al+Si) = 0.961), C_K did not increase compared to that at 250 ppmv K_2CO_3. At the same time, X_K decreased from 80.6 % to 40.8 %, indicating that more K_2CO_3 stayed unreacted with kaolin. This is probably because, as indicated by the equilibrium calculation, a complete conversion of kaolin

to K-aluminosilicate has taken place, at 250 ppmv K_2CO_3. Thereby, the increased K_2CO_3 was not captured by kaolin forming K-aluminosilicates at 375 and 500 ppmv K_2CO_3.

Impact of reaction temperature

The influence of reaction temperature on the K_2CO_3-capture reaction by kaolin was investigated experimentally at 800-1450 °C. The K_2CO_3 concentration was kept constant at 250 ppmv (500 ppmv K in flue gas), with a gas residence time of 1.2 s. The experimental C_K and X_K are compared with the equilibrium calculation results in Figure 3. It is seen that C_K increased from 0.159 g K/(g additive) to 0.231 g K/(g additive) by 31.1 %, when the reaction temperature increased from 800 °C to 1300 °C. Simultaneously, X_K increased from 59.3 % to 86.1 %. Whereas, when the reaction temperature increased further to 1450 °C, the C_K and X_K decreased slightly to 0.204 g K/(g additive) and 66.1 %, respectively. This is likely due to the change of reaction products. Equilibrium calculation suggests a decreased formation of kaliophilite ($KAlSiO_4$) and an increased formation of leucite ($KAlSi_2O_6$) at 1450 °C. However, leucite was not detected by XRD in the 1450 °C sample, probably because some amorphous K-species with K:Al:Si = 1:1:2 was formed. Considering the results on KOH-capture by kaolin in our previous study,[58] 900-1300 °C is a preferable temperature window for KOH and K_2CO_3 capture by kaolin.

3.3 KCl capture by kaolin

Equilibrium calculation

The results of equilibrium calculations of KCl capture by kaolin at different temperatures and KCl-concentrations were summarized in Table 3. Detailed results of the equilibrium calculation are available in Appendix III of the supporting information. The type of the K-aluminosilicate products formed varied with the molar K/(Al+Si) ratio in the reactants. As shown in Table 3, with a molar ratio

of K/(Al+Si) = 0.048 (50 ppmv KCl), the main K-aluminosilicate product was sanidine ($KAlSi_3O_8$) with a molar K:Al:Si ratio of 1:1:3. As the molar K/(Al+Si) ratio in reactants increased to 0.240 (250 ppmv KCl), leucite ($KAlSi_2O_6$) with a molar K:Al:Si ratio of 1:1:2, became the dominant K-aluminosilicate with some sanidine ($KAlSi_3O_8$) co-existing. When the molar ratio of K/(Al+Si) in reactants increased to 0.481 or higher (≥ 500 ppmv KCl), kaliophilite ($KAlSiO_4$) with a molar K:Al:Si ratio of 1:1:1 was predicted at the lower temperature range (800 - 900 °C), while at high temperatures (1100 - 1450 °C), leucite ($KAlSi_2O_6$) remained the dominant K-aluminosilicate.

Impact of potassium concentration

The impact of KCl concentration on the KCl-capture reaction by kaolin was investigated by EFR experiments using 50-1000 ppmv KCl and a reactor temperature of 1300 °C. The experimental C_K and X_K are compared with the equilibrium calculation results in Figure 4. The trend of the experimental C_K and X_K generally followed the equilibrium calculation data at 1300 °C. The C_K increased significantly from 0.020 g K/(g additive) to 0.131 g K/(g additive), when the KCl-concentration increased from 50 to 500 ppmv (K/(Al+Si) increased from 0.048 to 0.481 correspondingly). However, when the KCl-concentration increased further to 750 ppmv and 1000 ppmv (with a K/(Al+Si) molar ratio of 0.721 and 0.961, respectively), C_K did not increase. On the other hand, X_K decreased significantly from 90.1 % to about 25.3 % when the KCl-concentration increased from 50 ppmv to 1000 ppmv. This is probably because all the free Si has been consumed forming K-aluminosilicate at 500 ppmv KCl, with no Si available for further KCl capture. According to the equilibrium calculation, the main product of the KCl-kaolin reaction is leucite ($KAlSi_2O_6$), and the K-capture level is limited by the availability of Si. The formation of leucite was confirmed by the XRD analysis results, see Figure 6.

Impact of reaction temperature

To investigate the influence of reaction temperature on the KCl-capture reaction, experiments were conducted at temperatures from 800 °C to 1450 °C. In all experiments, the KCl concentration in flue gas was 500 ppmv, corresponding to a molar K/(Al+Si) ratio of 0.481 in reactants. The gas residence time was 1.2 s. The experimental results are compared to the equilibrium calculation results in Figure 5.

As shown in Figure 5 (A) and (B), at 500 ppmv KCl, the K-capture level (C_K) was close to the equilibrium prediction and stayed steady at about 0.142 g K/(g additive) at temperatures from 900 °C to 1300 °C. The K-conversion (X_K) was also steady at about 55.0 %. The C_K and X_K of KCl were lower than that of KOH capture by kaolin (C_K of KOH was 0.193 - 0.241 g K/(g additive), and X_K was 72.1 - 90.0 %). This could be explained that kaliophilite ($KAlSiO_4$) was detected by XRD in the KOH-reacted kaolin, while leucite ($KAlSi_2O_6$) was detected in the KCl-reacted kaolin (Figure 6). The formation of leucite consumed more Si than kaliophilite.

At 800 °C and 1450 °C, C_K was obviously lower than that at 900-1300 °C. At 800 °C, the reaction is probably kinetically controlled and do not reach the equilibrium state. Additionally, the incomplete vaporization of KCl at 800 °C, may also contribute to the low KCl conversion. At 1450 °C, the decrease of C_K may be due to an increased transformation of kaolin into mullite and amorphous silica,[39] which are less reactive towards KCl.[50] XRD analysis of calcinated kaolin samples in the EFR showed that the mullite formation became significant only above 1450 °C.

As shown in Figure 5 (A), C_K was also compared with the results from a study using a fixed bed reactor where cylindrical kaolin pellets of diameter of 1.5 mm was utilized for KCl capture.[50] The C_K values obtained in the fixed bed reactor are obviously lower than that in the EFR experiments, although the reaction time in the fixed bed reactor (about 1 hour) was much longer than that in the EFR (about 1 second). One possible reason is that in the fixed bed reactor it was actually mullite that reacted with KCl due to a long residence time of up to 1 hour. Another possible reason is that kaolin was in the

shape of pellets of 1.5 mm, where the reaction was strong controlled by internal diffusion. Another difference is that the results from fixed bed reactor have an opposite temperature-dependence trend comparing to that of the EFR. This is presumably because the controlling mechanisms in the two reactors are different. In the fixed bed experiments, the reaction was controlled by diffusion as mentioned above. Thus C_K decreased from 900 °C to 1300 °C, due to the increased sintering degree of kaolin pellets. However, C_K increased again when temperature was further increased to 1400 °C and 1500 °C, due to the enhanced inner diffusion caused by melting of kaolin pellets.[50] However, in the EFR, the reaction was mainly equilibrium controlled at 900 °C - 1300 °C. In summary, the favorable temperature window for KCl-capture by kaolin is 900-1300 °C.

Figure 5 (C) and (D) show that at 50 ppmv KCl, the experimental X_K and C_K were almost constant, and they generally followed the equilibrium predictions. The C_K was about 0.021 g K/(g additive) with about 80.2 % KCl captured by kaolin forming water-insoluble K-aluminosilicate.

The XRD spectra of water-washed KCl-reacted kaolin samples at 1300 °C and 1450 °C are compared in Figure 6. The results show that leucite ($KAlSi_2O_6$) was formed by the KCl-kaolin reaction at 1300 °C and 1450 °C. At 1450 °C, peaks of leucite are much stronger than that at 1300 °C. However, the ICP-OES analysis results showed than more leucite was formed at 1300 °C than experiments at 1450 °C. This indicates that a large amount of amorphous K-aluminosilicate was present in the 1300 °C product, and the leucite formed at 1450 °C was much more crystalline.

Impact of gas residence time

The impact of residence time on the KCl-capture reaction was studied at 1100 °C and 1300 °C. The KCl concentration in the flue gas was kept constant at 500 ppmv, with K/(Al+Si) = 0.481. The C_K and X_K results are shown in Figure 7.

The results in Figure 7 (A) and (B) show that at 1100 °C when the gas residence time increased from 0.8 s to 1.2 s, the C_K increased from 0.114 g K/(g additive) to 0.128 g K/(g additive) by 12.3 %. The X_K (K-conversion) increased from 42.4 % to 49.0 %. This indicates that at 1100 °C, the K-capture at residence time below 1.2 s is to some degree limited by kinetics or diffusion.

The results at 1300 °C show that the value of C_K and X_K did not change when the residence time increased from 0.6 s to 1.9 s and the number was close to the equilibrium prediction, implying that the KCl-capture reaction was at equilibrium. The results imply that at 1300 °C, with kaolin particles of D_{50} = 5.47 μm, it took very short time (≤ 0.6 s) for the KCl-capture reaction to reach equilibrium.

3.4 K_2SO_4 capture by kaolin

Equilibrium Calculation

The equilibrium calculation results of K_2SO_4 capture by kaolin at 25-500 ppmv K_2SO_4 (K-concentration was 50 ppmv to 1000 ppmv) are summarized in Table 4. Detailed results of the equilibrium calculation are available in Appendix IV of the supporting information. The type and amount of K-aluminosilicate formed changed with the K_2SO_4 concentration in flue gas (molar ratio of K/(Al+Si) in reactants). At 25 ppmv K_2SO_4 (molar ratio of K/(Al+Si) = 0.048), sanidine ($KAlSi_3O_8$) is predicted to be the main K-aluminosilicate product, with K:Al:Si = 1:1:3. At 125 ppmv K_2SO_4 (molar ratio of K/(Al+Si) = 0.240), leucite ($KAlSi_2O_6$) became the main K-aluminosilicate product, with sanidine ($KAlSi_3O_8$) co-existing. At 250, 375 and 500 ppmv K_2SO_4, (molar ratio of K/(Al+Si) ≥ 0.481), kaliophilite ($KAlSiO_4$) turned to be the main K-aluminosilicate product.

Impact of potassium concentration

The experimental K-capture level (C_K) and K-conversion (X_K) at 25-500 ppmv K_2SO_4 (50-1000 ppmv K) were compared with the equilibrium calculation results in Figure 8. Generally, the

experimental C_K and X_K were obviously lower than the equilibrium data, although they followed a similar trend. The experimental C_K increased from 0.018 g K/(g additive) to 0.115 g K/(g additive), when the K_2SO_4-concentration in flue gas increased from 25 ppmv to 250 ppmv. At the same time, the experimental X_K decreased from 68.0 % to 42.7 % correspondingly. As K_2SO_4-concentration increased further to 500 ppmv (K/(Al+Si) = 0.961), the C_K did not increase, while X_K decreased significantly to 21.7 %.

Impact of reaction temperature

The experimental C_K and X_K of K_2SO_4-capture by kaolin at different reaction temperatures from 800-1450 °C are compared with the equilibrium predictions in Figure 9. The results show that the experimental data did not follow the equilibrium predicted trend, and the experimental C_K and X_K were obviously lower than the equilibrium values. The experimental C_K and X_K increased significantly when the reaction temperature increased from 800 °C to 1100 °C. However, when the reaction temperature increased further to 1450 °C, the experimental C_K and X_K decreased slightly. This is because at temperatures below 1100 °C, the reaction was kinetically controlled, and the incomplete vaporization of K_2SO_4 at low temperatures also inhibited the conversion of K_2SO_4. At 1450 °C, the transformation of kaolin into mullite became significant, and the formed mullite is less reactive towards K_2SO_4.[50, 61] In summary, K_2SO_4 may be capture by kaolin most effectively at 900-1300 °C.

It is remarkable that the experimental C_K and X_K of K_2SO_4 are so much lower than the equilibrium predictions. But interestingly they were reasonably similar to the levels found for KCl, although the equilibrium predicted C_K and X_K for K_2SO_4 is considerably higher than that of KCl.

Kaliophilite ($KAlSiO_4$) was predicted as the main K-aluminosilicate product at 1100°C and 500 ppmv K (250 ppmv K_2SO_4) for K_2SO_4-capture reaction by kaolin. However, the XRD analysis results show that leucite ($KAlSi_2O_6$) was detected instead of kaliophilite ($KAlSiO_4$), see Figure 10. Thereby

the equilibrium product of K_2SO_4 capture by kaolin was wrongly predicted and the reaction product of K_2SO_4 capture by kaolin was the same as KCl.

3.5 Comparison of different K-species

The experimental results of using different K-species, including KOH, K_2CO_3, KCl and K_2SO_4, to react with kaolin at different K-concentration and different temperatures are compared in Figure 11. In Figure 11 (A), the experiments of KOH, K_2CO_3 and K_2SO_4 were all conducted at 1100 °C, while the KCl experiments were conducted at 1300 °C. However, the EFR experimental results (shown in Figure 5 (A)) indicate that KCl-capture by kaolin behaved similarly at 1100 °C and 1300 °C, so the results are still comparable.

The results show that KCl and K_2SO_4 were captured in a similar way, while KOH and K_2CO_3 behaved similarly. This is probably because the reaction between K_2CO_3 and kaolin took place according to reaction R3, R4 and R5. K_2CO_3 firstly decomposed into KOH and CO_2, and then the formed KOH reacted with kaolin forming K-aluminosilicate. The decomposition of K_2CO_3 has been observed in the K_2CO_3 vaporization and transformation experiments, which has been discussed in section 3.1.

$$K_2CO_3 + H_2O \rightarrow 2KOH + CO_2(g) \quad \text{(R 3)}$$

$$Al_2O_3 \cdot 2SiO_2 + 2KOH \rightarrow 2KAlSiO_4\ (kaliophilite) + 2H_2O \quad \text{(R 4)}$$

$$Al_2O_3 \cdot 2SiO_2 + 2SiO_2 + 2KOH \rightarrow 2KAlSi_2O_6\ (leucite) + 2H_2O \quad \text{(R 5)}$$

Another important result is that at 500 ppmv K in flue gas and above, KCl and K_2SO_4 are captured by kaolin less effectively compared to KOH or K_2CO_3. Although the equilibrium calculation predicted a similar K-capture level for K_2SO_4 and K_2CO_3 capture by kaolin at temperatures above 1100 °C. One reason is that at 500 ppmv K and above, kaliophilite ($KAlSiO_4$) was formed as product from KOH and

K_2CO_3 capture reaction, while leucite ($KAlSi_2O_6$) existed as the main K-aluminosilicate product from KCl and K_2SO_4 capture experiments, which has been confirmed by the XRD analysis. More Si was consumed in the KCl and K_2SO_4 capture reaction due to the formation of leucite ($KAlSi_2O_6$). Another reason is that the presence of HCl and SO_2 in KCl and K_2SO_4 capture reactions inhibited the K-capture reaction by kaolin, similar phenomena was observed in a previous sodium capture study.[51] The results indicate that more Al-Si based additive shall be used in boilers if Cl-rich fuels are fired and all K shall be converted to K-aluminosilicate. Additionally, an Al-Si additive with a relatively higher content of Si (like Si-rich coal fly ash) seems more suitable for K-capture when burning Cl-rich biomass fuels.

The results also show that kaolin captured KCl slightly more effectively than K_2SO_4. This may be good news for the situation of co-firing straw and coal where KCl and K_2SO_4 both exist, since Al and Si from the co-fired coal can destroy the corrosive KCl more effectively, and the less corrosive K_2SO_4 is captured at a lower level.

4 Conclusions

A thorough understanding of the K-capture reaction by kaolin under suspension-firing conditions is wanted to mitigate alkali-related problems in biomass combustion boilers. The reaction of KOH, K_2CO_3, KCl and K_2SO_4 capture by kaolin was studied by entrained flow reactor experiments and equilibrium calculations. The influence of molar ratio of K/(Al+Si) in reactants, K-concentration in flue gas, reaction temperature, K-species type, and residence time on the K-capture reaction was investigated.

The experimental results of using different K-concentrations show that for KCl at 1300 °C, and for KOH, K_2CO_3 and K_2SO_4 at 1100 °C, the K-capture level (C_K) increased when the K-concentration

increased from 50 ppmv to 500 ppmv (molar ratio K/(Al+Si) increased from 0.048 to 0.481). But it did not increase, when the K-concentration increased further to 750 ppmv and 1000 ppmv (molar ratio of K/(Al+Si) in reactants was 0.721 and 0.961), probably because all active compound in kaolin had already been converted forming K-aluminosilicates.

For KCl, KOH and K_2CO_3, C_K and X_K generally followed the equilibrium predictions at temperatures above 1100 °C, when applying a kaolin particle size of D_{50} = 5.47 μm and a residence time of 1.2 s. However, at lower temperatures (800 °C and 900 °C), the reactions were probably kinetically controlled, and the measured K-capture level was lower than the equilibrium predictions. For K_2SO_4, the measured C_K was significantly lower than the equilibrium predictions even at temperatures above 1100 °C. This is most likely because kaliophilite ($KAlSiO_4$) was predicted by the equilibrium calculations, but XRD analysis revealed that leucite ($KAlSi_2O_6$) was formed from the reaction. The KCl-capture experiments conducted with different residence times show that, at 1100 °C, the K-capture level increased slightly with residence time, indicating a kinetically limited reaction at this temperature. However, at 1300 °C, C_K reached the equilibrium level at a residence time as short as 0.6 s.

Experiments using different K-species show that, K_2CO_3 behaved the same as KOH in terms of being captured by kaolin at suspension fired conditions. KCl and K_2SO_4 behaved similarly, but they were captured less effectively than KOH and K_2CO_3. The study indicates that the main product of the KCl and K_2SO_4 reactions with kaolin when excess potassium is available are $KAlSi_2O_6$ (leucite) while $KAlSiO_4$ (kaliophilite) is mainly formed when KOH and K_2CO_3 reacted with kaolin with excess potassium available. The maximum obtainable K-capture level (C_K) for KCl and K_2SO_4 was approximately 0.12 g K/g kaolin while for KOH and K_2CO_3 a maximum capture level of approximately 0.24 g K/g kaolin could be obtained. The results imply that more kaolin shall be used in boilers if Cl-

rich fuels are fired and all K shall be converted to K-aluminosilicate. In addition, an Al-Si additive with a relatively higher content of Si (like Si-rich coal fly ash) may be more effective for K-capture when burning Cl-rich biomass fuels.

5 Acknowledgements

This work is part of the project 'Flexible use of Biomass on PF fired power plants' funded by Energinet.dk through the ForskEL programme, Ørsted Bioenergy & Thermal Power A/S and DTU.

Supporting Information. Appendix I of the supporting information: Detailed experimental conditions of the EFR experiments; Appendix II of the supporting information: Complete results of the equilibrium calculations of K_2CO_3 capture by kaolin. Appendix III of the supporting information: Complete results of the equilibrium calculations of KCl capture by kaolin. Appendix IV of the supporting information: Complete results of the equilibrium calculations of K_2SO_4 capture by kaolin.

6 References

(1) The Danish Government. *Our Future Energy*: Denmark, **2011**.
(2) Wu, H.; Glarborg, P.; Frandsen, F. J.; Dam-Johansen, K.; Jensen, P. A. *Energy Fuels* **2011**, 25, 2862-2873.
(3) Frandsen, F. J. *Fuel* **2005**, 84, 1277-1294.
(4) Sander, B. *Biomass Bioenergy* **1997**, 12, 177-183.
(5) Gao, X.; Yani, S.; Wu, H. *Energy Fuels* **2015**, 29, 5171-5175.
(6) Hansen, S. B.; Jensen, P. A.; Frandsen, F. J.; Wu, H.; Bashir, M. S.; Wadenbäck, J.; Sander, B.; Glarborg, P. *Energy Fuels* **2014**, 28, 3539-3555.
(7) Bashir, M. S.; Jensen, P. A.; Frandsen, F. J.; Wedel, S.; Dam-johansen, K.; Wadenba, J.; Pedersen, S. T. *Energy Fuels* **2012**, 26, 2317-2330.
(8) Laxminarayan, Y.; Jensen, P. A.; Wu, H.; Frandsen, F. J.; Sander, B.; Glarborg, P. *Energy Fuels* **2017**, 31, 8733-8741.
(9) Baxter, L. L. *Biomass Bioenergy* **1993**, 4, 85-102.
(10) Bashir, M. S.; Jensen, P. A.; Frandsen, F. J.; Wedel, S.; Dam-johansen, K.; Wadenba, J. *Energy Fuels* **2012**.
(11) Okoro, S. C.; Montgomery, M.; Frandsen, F. J.; Pantleon, K. *Energy Fuels* **2014**, 28, 6447-6458.
(12) Sandberg, J.; Karlsson, C.; Fdhila, R. B. *Appl. Energy* **2011**, 88, 99-110.
(13) Kling, Å.; Andersson, C.; Myringer, Å.; Eskilsson, D.; Järås, S. G. *Appl. Catal., B: Environ.* **2007**, 69, 240-251.
(14) Zheng, Y.; Jensen, A. D.; Johnsson, J. E.; Thøgersen, J. R. *Appl. Catal., B: Environ.* **2008**, 83, 186-194.
(15) Zheng, Y.; Jensen, A. D.; Johnsson, J. E. *Ind. Eng. Chem. Res.* **2004**, 43, 941-947.
(16) Jensen, P. A.; Frandsen, F. J.; Hansen, J.; Dam-Johansen, K.; Henriksen, N.; Hörlyck, S. *Energy Fuels* **2004**, 18, 378-384.
(17) Wu, H.; Bashir, M. S.; Jensen, P. A.; Sander, B.; Glarborg, P. *Fuel* **2013**, 113, 632-643.
(18) Baxter, L. L.; Miles, T. R.; Jenkins, B. M.; Milne, T.; Dayton, D.; Bryers, R. W.; Oden, L. L. *Fuel Process. Technol.* **1998**, 54, 47-78.
(19) Sippula, O.; Lind, T.; Jokiniemi, J. *Fuel* **2008**, 87, 2425-2436.
(20) Wiinikka, H.; Gebart, R.; Boman, C.; Boström, D.; Nordin, A.; Öhman, M. *Combust. Flame* **2006**, 147, 278-293.
(21) Blomberg, T. *Mater. Corros.* **2006**, 57, 170-175.
(22) Wang, G.; Shen, L.; Sheng, C. *Energy Fuels* **2012**, 26, 102-111.
(23) Niu, Y.; Tan, H.; Hui, S. e. *Prog. Energy Combust. Sci.* **2016**, 52, 1-61.
(24) Glarborg, P.; Marshall, P. *Combust. Flame* **2005**, 141, 22-39.
(25) Lindberg, D.; Backman, R.; Chartrand, P. *The Journal of Chemical Thermodynamics* **2007**, 39, 1001-1021.
(26) Nielsen, H. P.; Frandsen, F. J.; Dam-Johansen, K.; Baxter, L. L. *Prog. Energy Combust. Sci.* **2000**, 26, 283-298.
(27) Frandsen, F. J. Ash Formation , Deposition and Corrosion When Utilizing Straw for Heat and Power Production. Doctoral Thesis, Technical University of Denmark, 2011.
(28) Bashir, M. S.; Jensen, P. A.; Frandsen, F.; Wedel, S.; Dam-Johansen, K.; Wadenbäck, J.; Pedersen, S. T. *Fuel Process. Technol.* **2012**, 97, 93-106.

(29) Skrifvars, B.-J.; Laurén, T.; Hupa, M.; Korbee, R.; Ljung, P. *Fuel* **2004**, 83, 1371-1379.
(30) Damoe, A. J.; Wu, H.; Frandsen, F. J.; Glarborg, P.; Sander, B. *Energy Fuels* **2014**, 28, 3217-3223.
(31) Wang, L.; Skjevrak, G.; Hustad, J. E.; Skreiberg, Ø. *Energy Fuels* **2014**, 28, 208-218.
(32) Punjak, W. A.; Uberoi, M.; Shadman, F. *AlChE J.* **1989**, 35, 1186-1194.
(33) Xu, L.; Liu, J.; Kang, Y.; Miao, Y.; Ren, W.; Wang, T. *Energy Fuels* **2014**, 28, 5640-5648.
(34) Liao, Y.; Wu, S.; Chen, T.; Cao, Y.; Ma, X. *Energy Procedia* **2015**, 75, 124-129.
(35) Ahmaruzzaman, M. *Prog. Energy Combust. Sci.* **2010**, 36, 327-363.
(36) Punjak, W. A.; Shadman, F. *Energy Fuels* **1988**, 2, 702-708.
(37) Wang, M. R.; Jia, D. C.; He, P. G.; Zhou, Y. *Mater. Lett.* **2010**, 64, 2551-2554.
(38) Insley, H.; Ewell, R. H. *J. Res. Natl. Bur. Stand* **1935**, 14, 615-27.
(39) Tran, K.-Q.; Iisa, K.; Steenari, B.-M.; Lindqvist, O. *Fuel* **2005**, 84, 169-175.
(40) Tran, K.-Q.; Iisa, K.; Hagström, M.; Steenari, B.-M.; Lindqvist, O.; Pettersson, J. B. C. *Fuel* **2004**, 83, 807-812.
(41) Tran, Q. K.; Steenari, B.-M.; Iisa, K.; Lindqvist, O. *Energy Fuels* **2004**, 18, 1870-1876.
(42) Chen, Y.; Wang, G.; Sheng, C. *Energy Fuels* **2013**, 28, 136-145.
(43) Yao, Z. T.; Ji, X. S.; Sarker, P. K.; Tang, J. H.; Ge, L. Q.; Xia, M. S.; Xi, Y. Q. *Earth-Science Reviews* **2015**, 141, 105-121.
(44) Vassilev, S. V.; Vassileva, C. G. *Fuel* **2007**, 86, 1490-1512.
(45) Shaheen, S. M.; Hooda, P. S.; Tsadilas, C. D. *Journal of Environmental Management* **2014**, 145, 249-267.
(46) Blissett, R. S.; Rowson, N. A. *Fuel* **2012**, 97, 1-23.
(47) Davidsson, K. O.; Steenari, B. M.; Eskilsson, D. *Energy Fuels* **2007**, 21, 1959-1966.
(48) Bashir, M. S. Characterization and Quantification of Deposit Build-up and Removal in Straw Suspension-Fired Boilers. Technical University of Denmark, 2012.
(49) Uberoi, M.; Punjak, W. A.; Shadman, F. *Prog. Energy Combust. Sci.* **1990**, 16, 205-211.
(50) Zheng, Y.; Jensen, P. A.; Jensen, A. D. *Fuel* **2008**, 87, 3304-3312.
(51) Mwabe, P. O.; Wendt, J. O. L. Mechanisms governing trace sodium capture by kaolinite in a downflow combustor, In *26th Symposium on Combustion*, Napoli Italy, 1996.
(52) Punjak, W. A. High temperature interactions of alkali vapors with solids during coal combusiton and gasification. Ph.D., The University of Arizona, 1988.
(53) Shadman, F.; Punjak, W. A. *Thermochim. Acta* **1988**, 131, 141-152.
(54) Damoe, A. J.; Jensen, P. A.; Frandsen, F. J.; Wu, H.; Glarborg, P. *Energy Fuels* **2017**, 31, 555-570.
(55) Wang, L.; Skreiberg, Ø.; Becidan, M. *Appl. Therm. Eng.* **2014**, 70, 1262-1269.
(56) Steenari, B. M.; Lindqvist, O. *Biomass Bioenergy* **1998**, 14, 67-76.
(57) Mwabe, P. O. Mechanisms governing alkali metal capture by kaolinite in a downflow combustor. Ph.D. Thesis, The University of Arizona, 1993.
(58) Wang, G.; Jensen, P. A.; Wu, H.; Frandsen, F. J.; Sander, B.; Glarborg, P. *Energy Fuels* **2018**, Potassium Capture by Kaolin, Part 1: KOH, DOI: 10.1021/acs.energyfuels.7b03645.
(59) Bale, C. W.; Chartrand, P.; Degterov, S. A.; Eriksson, G.; Hack, K.; Ben Mahfoud, R.; Melançon, J.; Pelton, A. D.; Petersen, S. *Calphad.* **2002**, 26, 189-228.
(60) Bale, C. W.; Bélisle, E.; Chartrand, P.; Decterov, S. A.; Eriksson, G.; Hack, K.; Jung, I. H.; Kang, Y. B.; Melançon, J.; Pelton, A. D.; Robelin, C.; Petersen, S. *Calphad.* **2009**, 33, 295-311.
(61) Gale, T. K.; Wendt, J. O. L. *Aerosol Sci. Technol.* **2003**, 37, 865-876.

FIGURES

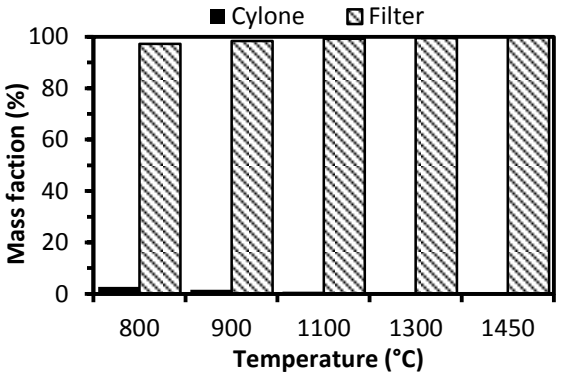

(A) K_2CO_3 vaporization in EFR

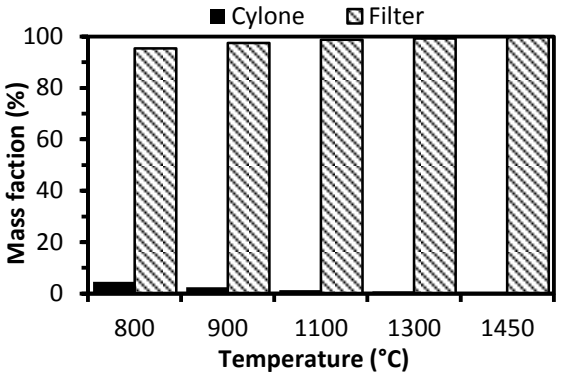

(B) KCl vaporization in EFR

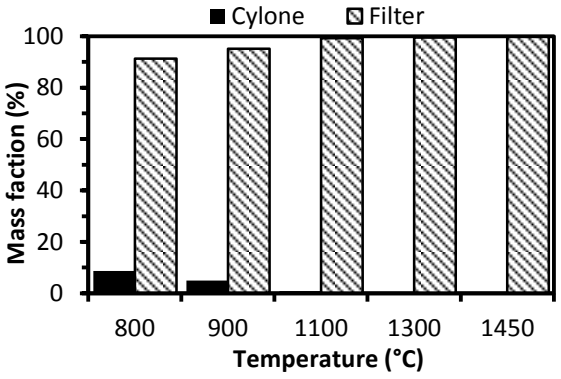

(C) K_2SO_4 vaporization in EFR

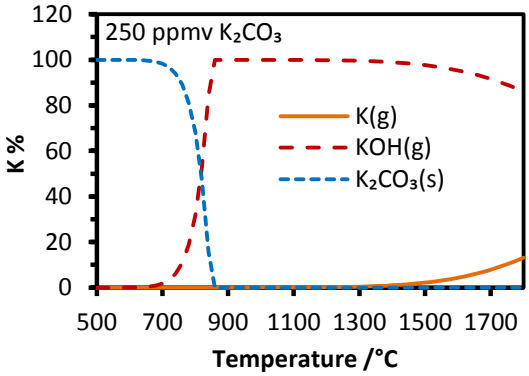

(D) Equilibrium calculation (K_2CO_3)

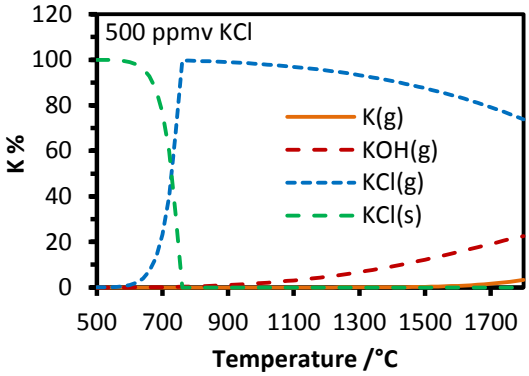

(E) Equilibrium calculation (KCl)

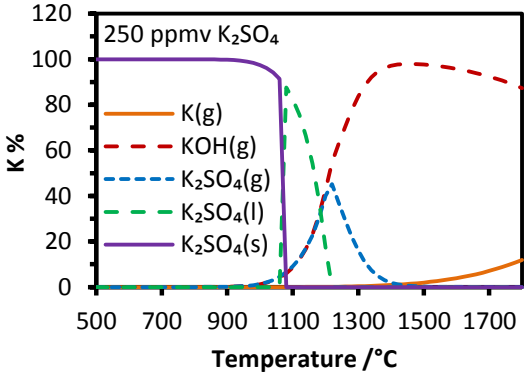

(F) Equilibrium calculation (K_2SO_4)

Figure 1. Mass distribution of solid samples collected in the cyclone and filter from K-salt vaporization experiments (A) K_2CO_3 (B) KCl (C) K_2SO_4, and corresponding equilibrium calculation results (D) K_2CO_3 (E) KCl (F) K_2SO_4.

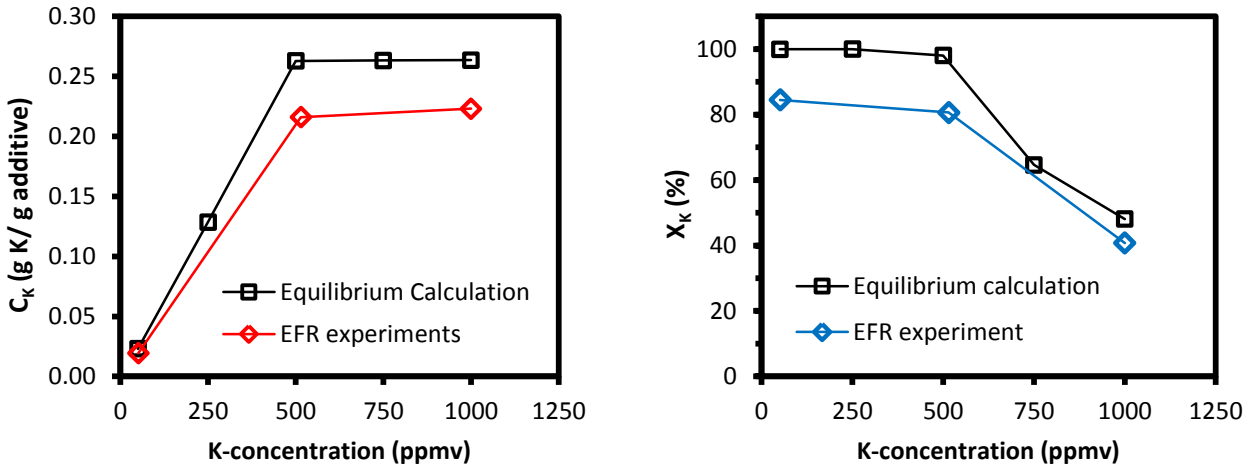

(A) K-capture level (C_K) (B) K-conversion (X_K)

Figure 2. K-capture level (C_K) and K conversion (X_K) of K_2CO_3-capture by kaolin at K_2CO_3 concentration varied from 25 ppmv to 500 ppmv (molar ratio of K/(Al+Si) in reactants changed from 0.048 to 0.961). Reaction temperature was 1100 °C. Gas residence time was 1.2 s. Equilibrium calculation results were included for comparison.

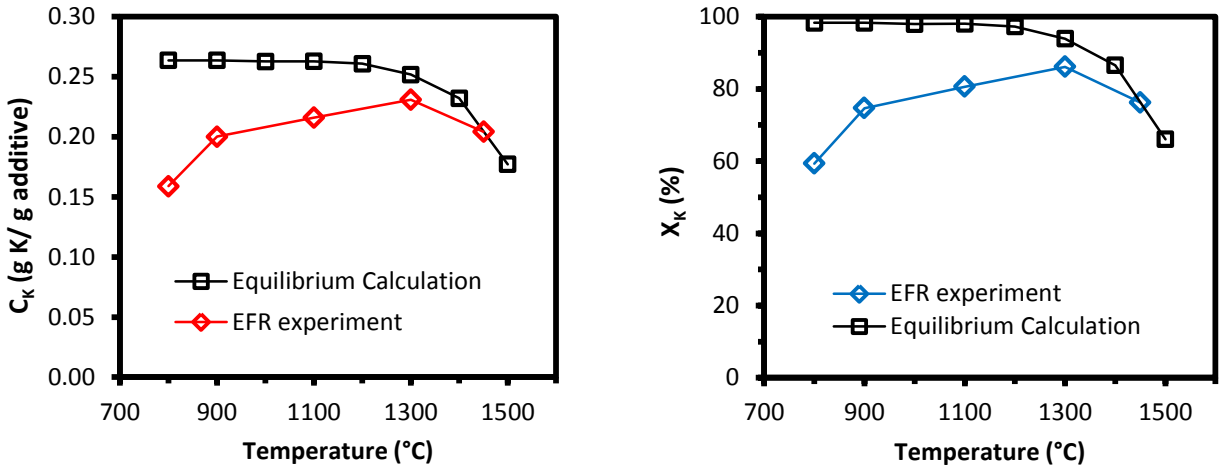

(A) K-capture level (C_K) (B) K-conversion (X_K)

Figure 3. K-capture level (C_K) and K-conversion (X_K) of K_2CO_3 capture by kaolin at different temperatures (800-1450 °C). K_2CO_3 concentration was 250 ppmv, molar ratio of K/(Al+Si) in reactants was 0.481, residence time was 1.2 s. Equilibrium calculation results are included for comparison.

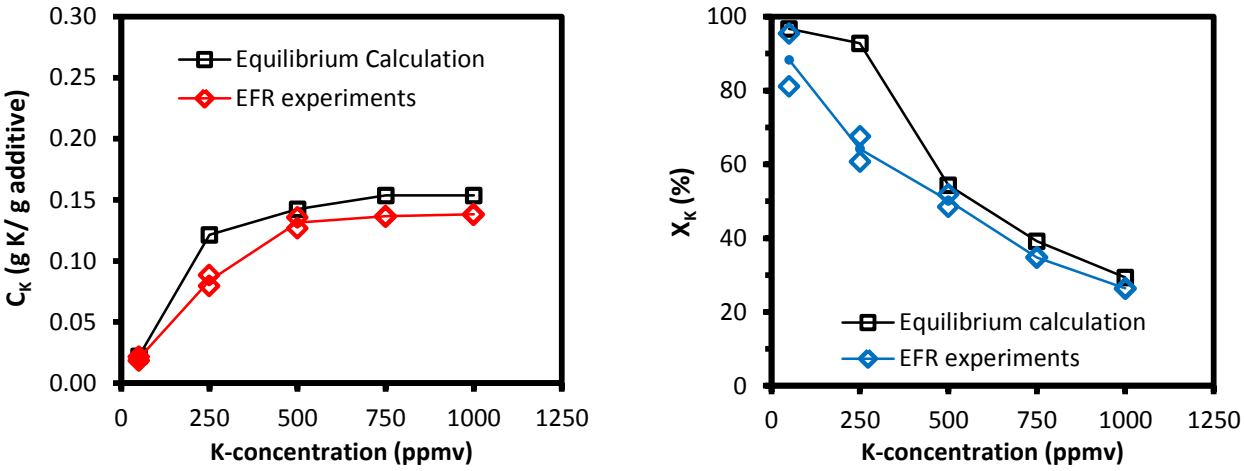

(A) K-capture level (C_K)

(B) K-conversion (X_K)

Figure 4. K-capture level (C_K) and K-conversion (X_K) of KCl capture by kaolin at 50 - 1000 ppmv KCl, the corresponding molar K/(Al+Si) ratio varied from 0.048 to 0.961, reaction temperature was 1300 °C. Gas residence time at 1300 °C was 1.0 s, and others were 1.2 s. Equilibrium calculation results are included for comparison.

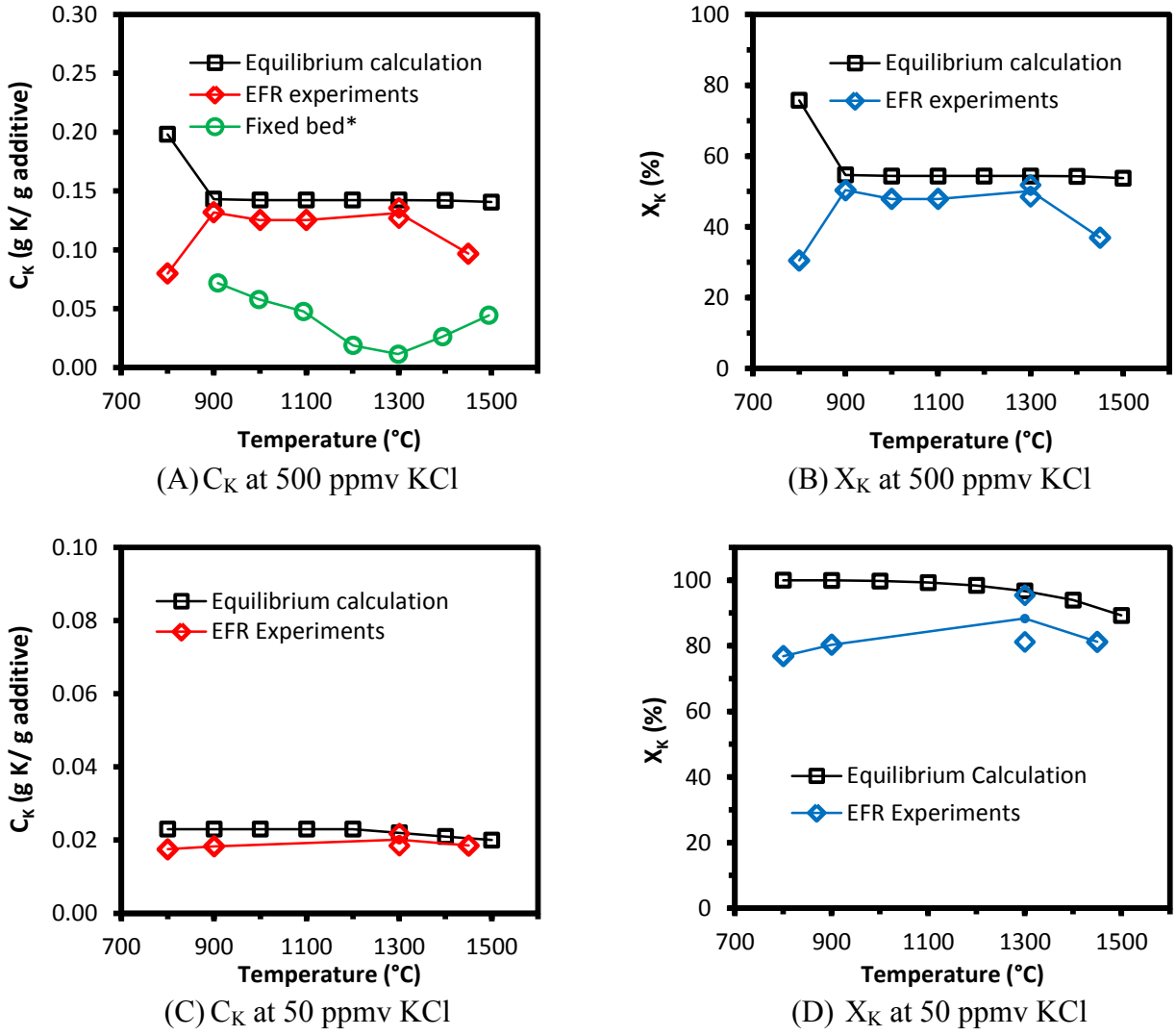

(A) C_K at 500 ppmv KCl

(B) X_K at 500 ppmv KCl

(C) C_K at 50 ppmv KCl

(D) X_K at 50 ppmv KCl

Figure 5. C_K (K-capture level) and X_K (K-conversion) of KCl capture by kaolin at different temperatures (800-1450 °C). KCl-concentration was 500 ppmv in (A) and (B), and it was 50 ppmv in (C) and (D). The gas residence time at 1300 °C was 1.0 s, others were 1.2 s. * Fixed bed data (1100 °C, 1000 ppmv KCl, residence time was 1 hour) is calculated from literature.[50]

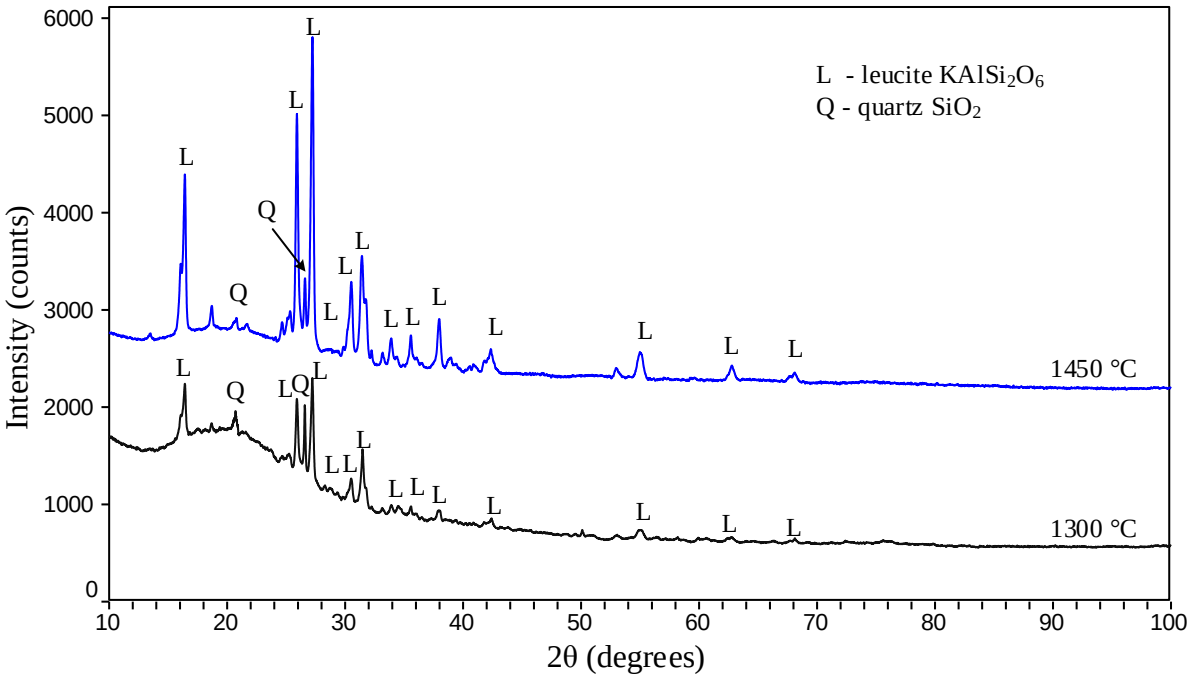

Figure 6. XRD spectra of water-washed KCl-reacted kaolin samples at 1300 °C and 1450 °C, KCl concentration in flue gas was 500 ppmv, molar K/(Al+Si) ratio in reactants was 0.481, gas residence time was 1.0 s and 1.2 s at 1300 °C and 1450 °C, respectively.

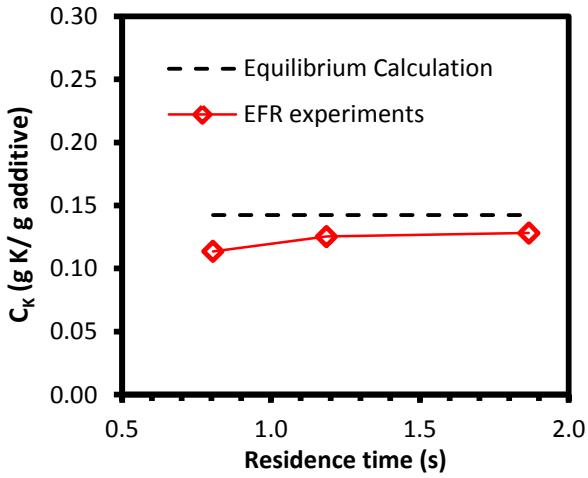

(A) K-capture level C_K at 1100 °C

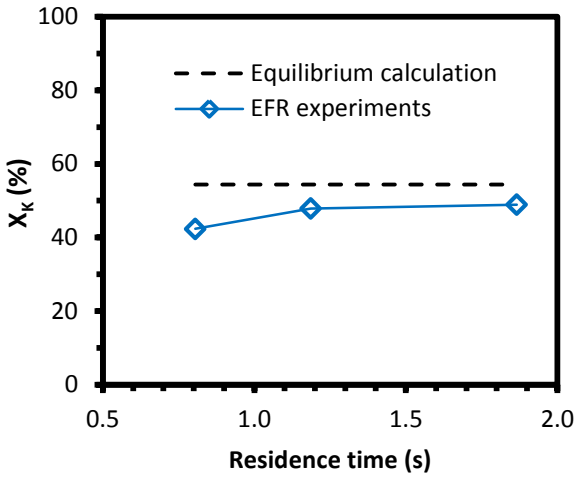

(B) K-conversion X_K at 1100 °C

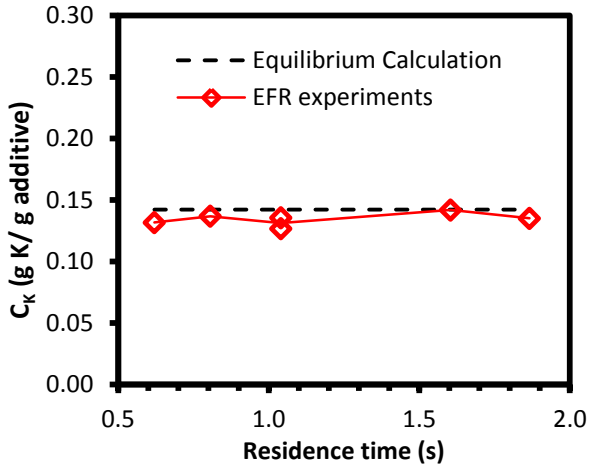

(C) K-capture level (C_K) at 1300 °C

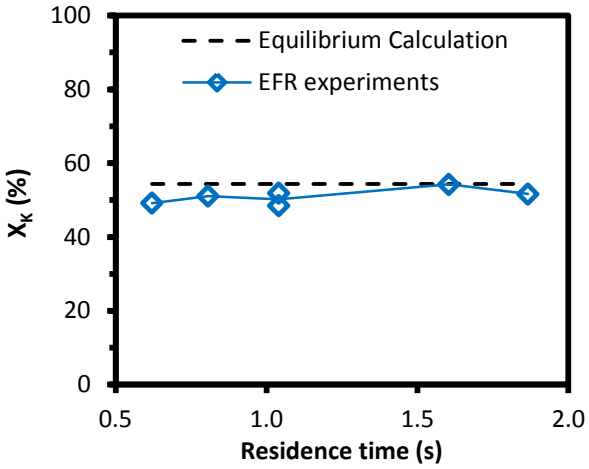

(D) K-conversion (X_K) at 1300 °C

Figure 7. K-capture level (C_K) and K-conversion (X_K) of KCl capture by kaolin at different residence time. KCl concentration in flue gas was 500 ppmv, (molar K/(Al+Si) ratio in reactants was 0.481). Reaction temperature was 1100 °C and 1300 °C.

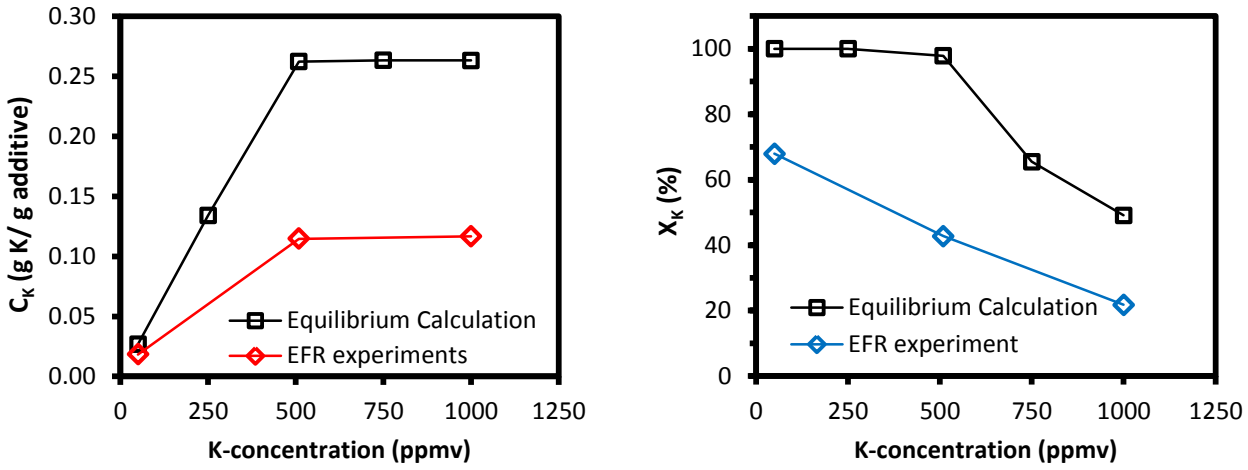

(A) K-capture level (C_K) (B) K-conversion (X_K)

Figure 8. C_K (K-capture level) and X_K (K-conversion) of K_2SO_4 capture by kaolin at 25-500 ppmv K_2SO_4 (50-1000 ppmv K) in flue gas (molar ratio of K/(Al+Si) in reactants varied from 0.048 to 0.961). Reaction temperature was 1100 °C. Gas residence time was 1.2 s. Equilibrium calculation results were included for comparison.

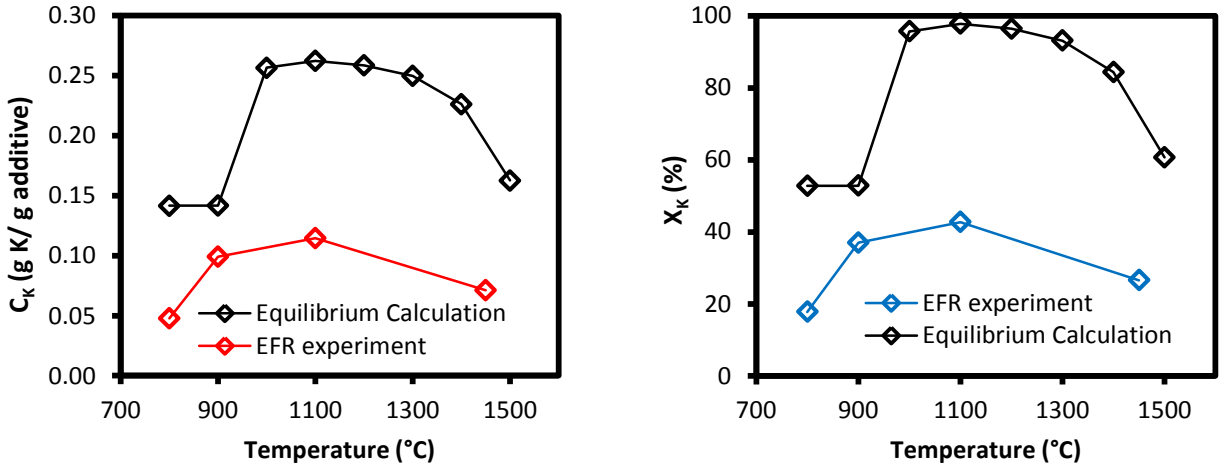

(A) K-capture level (C_K) (B) K-conversion (X_K)

Figure 9. K-capture level (C_K) and K-conversion (X_K) of K_2SO_4 capture by kaolin at 800-1450 °C. K_2SO_4 concentration was 250 ppmv (500 ppmv K). Residence time was 1.2 s. Equilibrium calculation results are included for comparison.

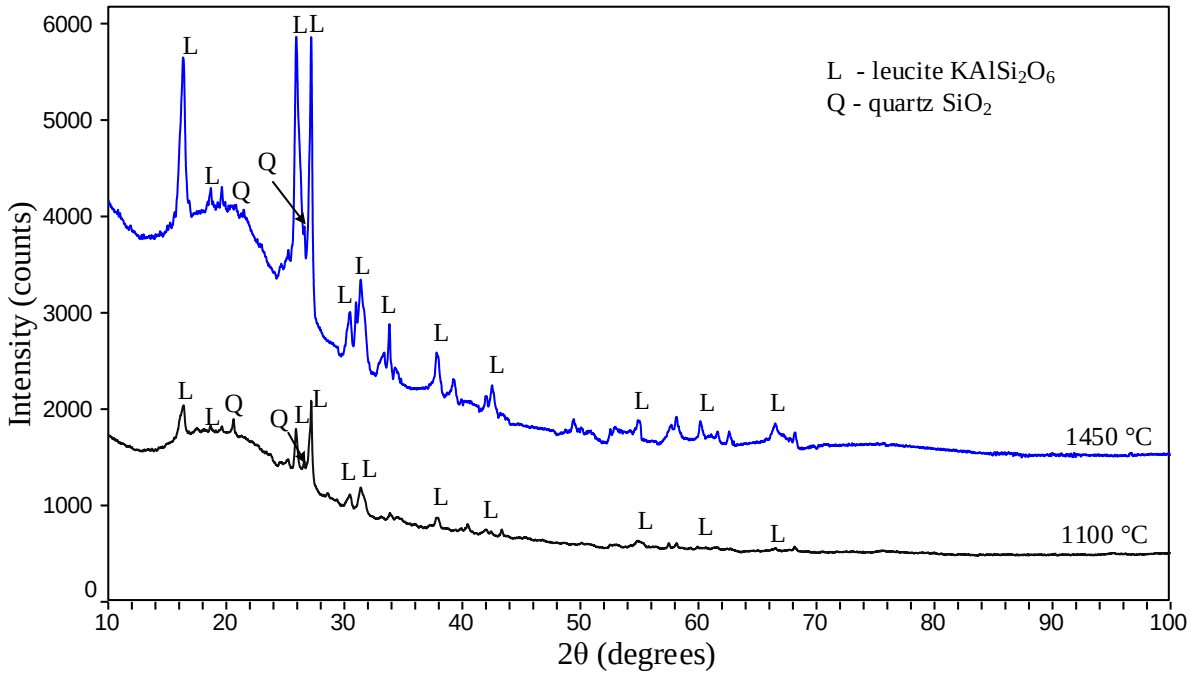

Figure 10. XRD spectra of water-washed K_2SO_4-reacted kaolin at 1100 °C and 1450 °C. K_2SO_4 concentration was 250 ppmv (500 ppmv K) in flue gas. Molar K/(Al+Si) ratio in reactants was 0.481. Gas residence time was 1.2 s.

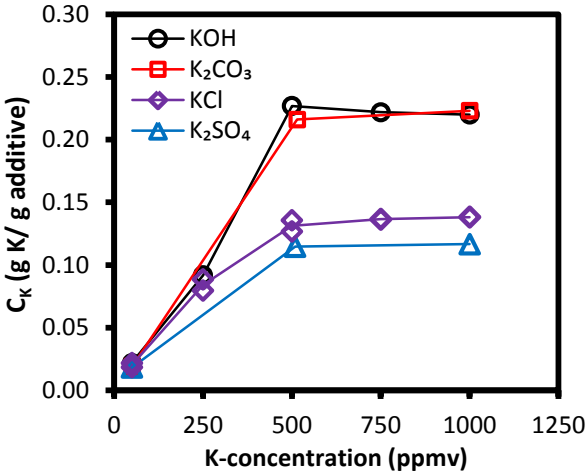

(A) C_K at different K-concentrations

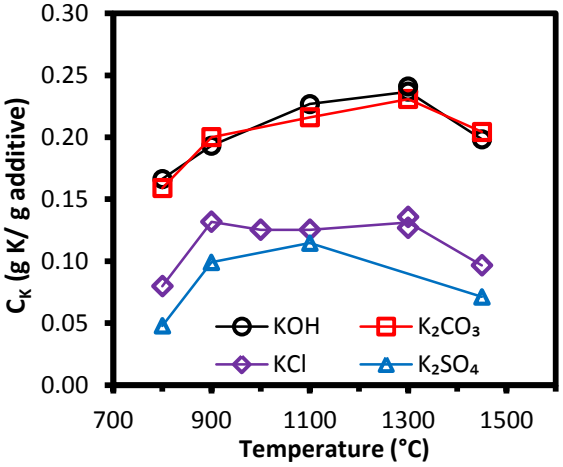

(B) C_K at different temperatures

Figure 11. Comparison of KOH, K_2CO_3, KCl, and K_2SO_4 capture by kaolin at different K-concentrations and temperatures. In (A), KOH, K_2CO_3 and K_2SO_4 experiments were at 1100 °C, KCl experiments were at 1300 °C. In (B), K-concentration was 500 ppmv for all experiments.

TABLES

Table 1. Characteristics of kaolin powder.

Properties	Kaolin
O (wt.%, dry)	56.9
S (wt.%, dry)	0.02
Si (wt.%, dry)	22.0
Al (wt.%, dry)	19.0
Fe (wt.%, dry)	0.47
Ca (wt.%, dry)	0.1
Mg (wt.%, dry)	0.14
Na (wt.%, dry)	0.1
K (wt.%, dry)	1.1
Ti (wt.%, dry)	0.02
P (wt.%, dry)	0.05
Cl (wt.%, dry)	0.1
D_{50} (μm)	5.47
BET surface area (m^2/g)	12.70

Table 2. Experimental conditions of the EFR experiments.

Experimental series	**K-species**	**Additives**	**Temp./°C**	**Gas residence time/s**	**K in gas /ppmv**	**K/(Al+Si)**
(A) K-salt vaporization experiments	K_2CO_3	No additive	800, 900, 1100, 1300, 1450	1.2	500	No Al, Si
	KCl					
	K_2SO_4					
(B) K_2CO_3-capture by kaolin (impact of **K-concentration**)	K_2CO_3	kaolin	1100	1.2	50	0.048
					500	0.481
					1000	0.961
(C) K_2CO_3-capture by kaolin (impact of **temperature**)	K_2CO_3	kaolin	800	1.2	500	0.481
			900			
			1100			
			1300			
			1450			
(D) KCl-capture by kaolin (impact of **K-concentration**)	KCl	kaolin	1300	1.0-1.2	50*	0.048
					250*	0.240
					500*	0.481
					750	0.721
					1000	0.961
(E) KCl-capture by kaolin (impact of **temperature**)	KCl	kaolin	800	1.0-1.2	50, 500	0.048, 0.481
			900			
			1100			
			1300*			
			1450			
(F) KCl-capture by kaolin (impact of **residence time**)	KCl	kaolin	1100, 1300	0.6	500	0.481
				0.8		
				1.2		
				1.9		
(G) K_2SO_4-capture by kaolin (impact of **K-concentration**)	K_2SO_4	kaolin	1100	1.2	50	0.048
					500	0.481
					1000	0.961
(H) K_2SO_4-capture by kaolin (impact of **temperature**)	K_2SO_4	kaolin	800	1.2	500	0.481
			900			
			1100			
			1450			

Note: *Experiments were repeated.

Table 3. Results of equilibrium calculations of KCl-capture by kaolin.

Input conditions	Temp. /°C	K-species appearing	Al-con.	Si-con.	K-con.	K-capture/(g K/g additive)
50 ppmv KCl, K/(Al+Si) =0.048	800	100 % $KAlSi_3O_8$	9 %	24 %	100 %	0.023
	900	100 % $KAlSi_3O_8$	9 %	24 %	100 %	0.023
	1100	99 % $KAlSi_3O_8$ + 1 % KCl	9 %	24 %	99 %	0.023
	1300	97 % $KAlSi_3O_8$ + 3 % KCl	8 %	23 %	97 %	0.022
	1450	92 % $KAlSi_3O_8$ + 7 % KCl + 1 % KOH	8 %	22 %	92 %	0.022
250 ppmv KCl, K/(Al+Si) =0.240	800	21 % $KAlSi_3O_8$ + 79 % $KAlSi_2O_6$	50 %	98 %	100 %	0.131
	900	23 % $KAlSi_3O_8$ + 77 % $KAlSi_2O_6$ + 1 % KCl	50 %	98 %	99 %	0.130
	1100	28 % $KAlSi_3O_8$ + 70 % $KAlSi_2O_6$ + 3 % KCl	49 %	99 %	97 %	0.128
	1300	33 % $KAlSi_3O_8$ + 60 % $KAlSi_2O_6$ + 7 % KCl	46 %	97 %	93 %	0.121
	1450	45 % $KAlSi_3O_8$ + 41 % $KAlSi_2O_6$ + 13 % KCl	43 %	97 %	87 %	0.113
500 ppmv KCl, K/(Al+Si) =0.481	800	33 % $KAlSi_2O_6$ + 43 % $KAlSiO_4$ + 24 % KCl	75 %	100 %	76 %	0.198
	900	54 % $KAlSi_2O_6$ + 1 % $KAlSiO_4$ + 45 % KCl	54 %	100 %	55 %	0.143
	1100	54 % $KAlSi_2O_6$ + 46 % KCl	54 %	100 %	54 %	0.142
	1300	54 % $KAlSi_2O_6$ + 45 % KCl	54 %	100 %	54 %	0.142
	1450	54 % $KAlSi_2O_6$ + 45 % KCl + 1 % KOH	54 %	100 %	54 %	0.142
750 ppmv KCl, K/(Al+Si) =0.721	800	10 % $KAlSi_2O_6$ + 56 % $KAlSiO_4$ + 35 % KCl	98 %	100 %	65 %	0.256
	900	22 % $KAlSi_2O_6$ + 32 % $KAlSiO_4$ + 47 % KCl	80 %	100 %	53 %	0.209
	1100	38 % $KAlSi_2O_6$ + 62 % KCl	56 %	100 %	38 %	0.147
	1300	37 % $KAlSi_2O_6$ + 62 % KCl	56 %	100 %	37 %	0.147
	1450	37 % $KAlSi_2O_6$ + 61 % KCl + 1 % KOH	56 %	100 %	37 %	0.147
1000 ppmv KCl, K/(Al+Si) =0.961	800	4 % $KAlSi_2O_6$ + 47 % $KAlSiO_4$ + 49 % KCl	100 %	100 %	50 %	0.263
	900	6 % $KAlSi_2O_6$ + 42 % $KAlSiO_4$ + 52 % KCl	95 %	100 %	48 %	0.251
	1100	27 % $KAlSi_2O_6$ + 73 % KCl	54 %	100 %	27 %	0.142
	1300	27 % $KAlSi_2O_6$ + 72 % KCl + 1 % KOH	54 %	100 %	27 %	0.142
	1450	27 % $KAlSi_2O_6$ + 71 % KCl + 1 % KOH	54 %	100 %	27 %	0.142

Table 4. Equilibrium calculation results of K_2SO_4 capture by kaolin.

Input conditions	Temp. /°C	K-species appearing	Al-con.	Si-con.	K-con.	K-capture/(g K/g additive)
25 ppmv K_2SO_4, K/(Al+Si) = 0.048	800	100 % $KAlSi_3O_8$	10 %	28 %	100 %	0.027
	900	100 % $KAlSi_3O_8$	10 %	28 %	100 %	0.027
	1100	100 % $KAlSi_3O_8$	10 %	28 %	100 %	0.027
	1300	100 % $KAlSi_3O_8$	10 %	28 %	100 %	0.027
	1450	99 % $KAlSi_3O_8$ + 1 % KOH	10 %	28 %	99 %	0.026
125 ppmv K_2SO_4, K/(Al+Si) = 0.240	800	92 % $KAlSi_2O_6$ + 8 % $KAlSi_3O_8$	51 %	98 %	100 %	0.134
	900	92 % $KAlSi_2O_6$ + 8 % $KAlSi_3O_8$	51 %	98 %	100 %	0.134
	1100	93 % $KAlSi_2O_6$ + 7 % $KAlSi_3O_8$	51 %	97 %	100 %	0.134
	1300	93 % $KAlSi_2O_6$ + 7 % $KAlSi_3O_8$	51 %	96 %	100 %	0.134
	1450	94 % $KAlSi_2O_6$ + 5 % $KAlSi_3O_8$	51 %	96 %	100 %	0.133
250 ppmv K_2SO_4, K/(Al+Si) = 0.481	800	53 % $KAlSi_2O_6$ + 47 % K_2SO_4	54 %	100 %	53 %	0.142
	900	53 % $KAlSi_2O_6$ + 47 % K_2SO_4	54 %	100 %	53 %	0.142
	1100	7 % $KAlSi_2O_6$ + 90 % % $KAlSiO_4$ + 1 % KOH	100 %	99 %	98 %	0.262
	1300	13 % $KAlSi_2O_6$ + 80 % % $KAlSiO_4$ + 6 % KOH	95 %	100 %	93 %	0.250
	1450	31 % $KAlSi_2O_6$ + 44 % % $KAlSiO_4$ + 24 % KOH	76 %	100 %	75 %	0.201
375 ppmv K_2SO_4, K/(Al+Si) = 0.721	800	35 % $KAlSi_2O_6$ + 65 % K_2SO_4	54 %	99 %	35 %	0.141
	900	35 % $KAlSi_2O_6$ + 65 % K_2SO_4	54 %	100 %	35 %	0.142
	1100	5 % $KAlSi_2O_6$ + 61 % % $KAlSiO_4$ + 33 % K_2SO_4 + 2 % KOH	100 %	100 %	65 %	0.263
	1300	5 % $KAlSi_2O_6$ + 61 % % $KAlSiO_4$ + 5 % K_2SO_4 + 29 % KOH	100 %	100 %	65 %	0.263
	1450	5 % $KAlSi_2O_6$ + 61 % % $KAlSiO_4$ + 34 % KOH	100 %	100 %	65 %	0.263
500 ppmv K_2SO_4, K/(Al+Si) = 0.961	800	26 % $KAlSi_2O_6$ + 74 % K_2SO_4	54 %	100 %	26 %	0.141
	900	26 % $KAlSi_2O_6$ + 74 % K_2SO_4	54 %	100 %	26 %	0.142
	1100	4 % $KAlSi_2O_6$ + 45% % $KAlSiO_4$ + 50 % K_2SO_4 + 1 % KOH	100 %	100 %	49 %	0.263
	1300	4 % $KAlSi_2O_6$ + 45% % $KAlSiO_4$ + 14 % K_2SO_4 + 36 % KOH	100 %	100 %	49 %	0.263
	1450	4 % $KAlSi_2O_6$ + 45% % $KAlSiO_4$ + 1 % K_2SO_4 + 49 % KOH	100 %	100 %	49 %	0.263